Journal of Nuclear Medicine, published on October 12, 2017 as doi:10.2967/jnumed.116.187419

Advanced methods for radiolabelling nanomedicines for multi-modality nuclear/MR imaging

Jennifer Lamb and Jason P. Holland*

University of Zurich, Department of Chemistry, Winterthurerstrasse 190, CH-8057, Zurich, Switzerland

***Correspondence:**

Prof. Dr Jason P. Holland

Tel: +41.44.63.53.990

E-mail: jason.holland@chem.uzh.ch

First author: E-mail: jennifer.lamb@chem.uzh.ch. Tel: +41.44.63.53.995

Running Title: *Chelate-free radiochemistry*

Noteworthy:

- Effective design of multi-modality nanomedicines for nuclear/MR imaging requires new radiochemical methods to overcome limitations imposed by conventional prosthetic group and chelate-based chemistries (page 4)
- Chelate-free methods exploit intrinsic chemical properties of nanoparticles to effect facile and efficient radiolabelling (Page 10)
- Mechanistic principles underpinning seven distinct chelate-free radiolabelled methods are present (Page 10, Figure 3)

ABSTRACT

The advent of hybrid cameras that combine magnetic resonance imaging with either single-photon emission computed tomography (SPECT/MRI) or positron-emission tomography (PET/MRI) has stimulated growing interest in developing multi-modality imaging probes. Countless options are available for fusing magnetically active species with positron- or gamma-ray emitting radionuclides. The initial problem is one of choice: which chemical systems are a suitable basis for developing hybrid imaging agents? Any attempt to answer this question must also address how the physical, chemical, and biological properties of a unified imaging agent can be tailored to ensure that optimum specificity and contrast is achieved simultaneously for both imaging modalities. Nanoparticles have emerged as attractive platforms for building multi-modality SPECT/MRI and PET/MRI radiotracers. A wide variety of nanoparticle constructs have been utilised as radiotracers but irrespective of the particle class, radiolabelling remains a key step. Classical methods for radiolabelling nanoparticles involve functionalisation of the particle surface, core or coating. These modifications typically rely on using traditional metal ion chelate or prosthetic group chemistries. Though seemingly innocuous, appending nanoparticles with these radiolabelling handles can have dramatic effects on important properties such as particle size, charge and solubility. In turn, alterations in the chemical and physical properties of the nanoparticle often have a negative impact on their pharmacological profile. A central challenge in radiolabelling nanoparticles is to identify alternative chemical methods that facilitate the introduction of a radioactive nuclide without detrimental effects on the pharmacokinetic and toxicological properties of the construct. Efforts to solve this challenge have generated a range of innovative, ‘chelate-free’ radiolabelling methods that exploit intrinsic chemical features of nanoparticles. Here, the chemistry of nine mechanistically distinct methods for radiolabelling

nanoparticles is presented. This discourse illustrates the evolution of nanoparticle radiochemistry from classical approaches through to modern chelate-free or intrinsic methods.

KEYWORDS: nanoparticles, intrinsic radiolabelling, chelate-free, chemisorption, doping, isotopic exchange, cation exchange, PET/MRI.

INTRODUCTION

Nanomedicine is the application of nanotechnology to diagnose or treat disease (*1*). In the fields of radiochemistry and nuclear medicine, nanoparticles are gaining prominence as platforms for designing hybrid imaging and therapeutic agents (*2*–*5*). In particular, nanoparticle-based radiotracers show promise as multi-modality SPECT/MRI and PET/MRI probes. Reasons why nanoparticles have attracted attention can be ascribed to their unique physical and chemical characteristics. Enhanced rigidity, controlled shape and size, discrete charge and electromagnetic properties, high surface area to volume ratios, variable porosity, resistance to metabolism *in vivo*, and tuneable chemical reactivity at the surface, on coatings and inside the particle core are just some of the features that demarcate nanoparticles as highly versatile scaffolds.

In spite of their potential, there are many questions and challenges that must be addressed before nanoparticle-based imaging agents can cross the divide from preclinical to clinical applications. From a chemical standpoint, nanoparticle-based agents are highly complex. Average formulations contain particles with varying chemical composition including a range of sizes, variable drug loading densities, and differential presentation of targeting vectors in terms of their number per particle as well as their spatial location and 3-dimensional orientation. For this reason, most measurements made using nanoparticles rely on determination of the average properties of a bulk sample. Such inherent variability is a potential problem for ensuring batch-to-batch reproducibility and can induce differences in the biological properties of nanoparticles. Attention must be paid to ensure that parameters including the pharmacokinetic profile, cytotoxicity, target affinity and specificity remains consistent between formulations (*6*). It is easy to appreciate that whilst having access to such a wide range of physical and chemical parameters is beneficial from

a design perspective, controlling each part of a nanoparticle system to meet stringent current Good Manufacturing Practice regulations is a formidable task.

Considering the development of a single molecular imaging probe that can be used to acquire nuclear and magnetic resonance images simultaneously, a number of important design criteria must be incorporated into the final construct. For instance, a successful radiolabelled SPECT/MRI or PET/MRI probe should display high chemical, radiochemical and metabolic stability, low toxicity, and a favourable pharmacokinetic profile with rapid accumulation in the target regions matched by excretion from background organs (*7*). A crucial question that has yet to be answered in detail is how can one molecule fulfil the usual chemical and physical requirements of nuclear and magnetic imaging probes without compromising on target specificity or image contrast. This problem is highlighted by the acute difference in the normal administered concentrations between standard PET radiotracers and MRI contrast agents. Clinical-grade fluorine-18-labelled PET radiotracers have typical specific activities around 185 GBq/μmol (5 Ci/μmol) with administered radioactive doses in humans around 370 to 740 MBq (10 – 20 mCi) (*8*). For an average human male (~75 kg) the administered dose of radiotracer equates to around ~2 to 4 nmol (ca. 25 to 50 pmol/kg body weight). Typical gadolinium-based MRI contrast agents are administered at relatively high doses up to 0.2 mmol Gd per kg body weight (*9*). This represents a staggering ~7-orders of magnitude difference between the administered doses (and sensitivities) of PET and MRI imaging probes. How can a single, multi-modality PET/MRI radiotracer reconcile this difference in concentration whilst maintaining high contrast in MRI and avoiding target saturation which would reduce PET signal uptake and specificity? For a given combination of biological target and imaging probe, does a concentration range exist that would be an acceptable compromise for simultaneous PET/MRI (or SPECT/MRI)? At present, these questions have not

been addressed adequately. Most reports on multi-modality imaging agents have tended to decouple the nuclear and imaging components by showing that a single species (usually nanoparticles) administered at *different* doses can be applied for sequential SPECT/PET and MRI. Recent work by Zhao *et al.* is a notable exception (*10*). SPECT/MRI studies showed that a single-dose administration of iodine-125-radiolabelled human heavy-chain ferritin nanocages (^{125}I-M-HFn) could image HT-29 tumours at a dose of 18.5 MBq (500 μCi) of ^{125}I and 11.2 μg of Fe. However, it remains uncertain if a similar approach would be generally applicable to more diverse imaging biomarkers of low abundance.

Returning to the chemistry of nanoparticles, a practical consideration is that the radiolabelling step should be easy and reproducible. Ideally, radiolabelling should be performed in the final step of production, and addition of the radionuclide should not alter (or have known minimal effects on) the physical, chemical, and biological properties of the nanoparticle. These demanding requirements have led researchers to develop a number of innovative solutions for producing radiolabelled nanoparticles. In the following sections, the chemistry and application of nine, mechanistically distinct methods for radiolabelling different types of nanoparticles is explored. Classical radiolabelling methods based on modification of nanoparticles using metal ion chelation and prosthetic group chemistry is briefly introduced. The focus of this review is to illustrate how intrinsic chemical properties of nanoparticles are being harnessed by state-of-the-art 'chelate-free' radiolabelling methods to produce multi-modality imaging agents (*11*,*12*).

METHODS FOR RADIOLABELLING NANOPARTICLES

The following sections provide an overview of the types of chemistry that have been used to radiolabel nanoparticles (*11–13*).

Classical Radiolabelling 1: Particle Surface Modifications

Traditional approaches for radiolabelling nanoparticles rely on well-established radiochemical methods including the use of fluorine-18-based prosthetic groups or radiometal ion chelation. Here, nanoparticles are typically coated with surface reactive groups which serve a dual purpose. First, they allow covalent attachment of radionuclides *via* prosthetic groups or multidentate chelates. Second, they provide thermodynamically, kinetically, and metabolically stable anchors that ensure the radionuclide remains associated with nanoparticle *in vivo*. Three common examples of surface anchoring include thiol-mediate binding to Au-nanoparticles (*14–16*), silylation of surface hydroxyls (*17*), and bisphosphonate binding (*18*,*19*) to iron oxide particles (Figure 1).

In an archetype example, Guerrero *et al*. (*15*) produced ^{18}F-labelled Au-nanoparticles (AuNPs). The AuNPs were pre-functionalised with a cysteine-lysine diamino acid *via* covalent bonding of the thiolate to the Au surface. Radiolabelling was accomplished by attaching the fluorine-18 radiolabelled prosthetic group, *N*-succinimidyl-4-^{18}F-fluorobenzoate (^{18}F-SFB) *via* amide bond formation on the lysine side-chain. Rojas *et al*. (*17*) used a similar strategy but employed 3-(aminopropyl)triethoxysilane to decorate the surface of ceria (CeO_2) nanoparticle with a primary amine that was subsequently coupled to ^{18}F-SFB. A major drawback of this approach is that multiple radiolabelling steps are required, which limits overall radiochemical yields and specific activities. Others have sought to overcome these issues by developing a cysteamine derivative of ^{18}F-2-fluoro-2-deoxy-*d*-glucose (^{18}F-FDG-CA) that binds to AuNPs (*14*). Zhu *et al*. (*16*) also reported an interesting approach to make ^{18}F-radiolabelled PEGylated AuNPs that relied on Si-^{18}F bond formation. The thiol (4-(di-*tert*-butyl-^{18}F-fluorosilanyl)benzenethiol (^{18}F-SiFA-SH) was produced *via* ^{18}F/^{19}F isotopic exchange and was subsequently conjugated to maleimido-

AuNPs giving high radiochemical yields (60−87%). While this prosthetic group approach solves some of the issues associated with low RCYs, it is not clear how much of the ^{18}F-SiFA-SH reacts with the maleimido group and how much reacts directly with the AuNP surface.

In 2011, Rosales *et al*. used bisphosphonate chemistry to generate dual-modality SPECT/MRI and PET/MRI radiotracers based on conjugation of superparamagnetic iron oxide nanoparticles (SPIONs) with either ^{99m}Tc or ^{64}Cu, respectively (*18*,*19*). Bisphosphonates display well-established affinity for several different classes of inorganic surfaces including various metal oxides, and hydroxyapatite crystals found in bone. Both studies followed a similar approach in which multidentate chelates, chosen for their selectivity toward a particular radiometal ion, were functionalised with a bisphosphonate group. $^{64}Cu^{2+}$–*bis*(di-thiocarbamatebisphosphonate) and ^{99m}Tc-dipicolylamine(DPA)-alendronate were conjugated Endorem (Ferumoxide or Feridex) – dextran-coated magnetite (Fe_3O_4) nanoparticles (120–180 nm diameter) approved for T_2- or T_2*-contrast enhanced MRI (*20*). Detailed stability studies *in vitro* and multi-modality imaging *in vivo* confirmed the viability of bisphosphonate chemistry for radiolabelling metal oxides nanoparticles (*21*).

Classical Radiolabelling 2: Particle Coating Modifications

The second fundamental approach to radiolabelled nanoparticles involves modification to the particle coating. Radiolabelling reactions on particle coatings involve similar prosthetic group or chelate-based chemistries as described above. The key difference is that surface anchoring groups are not required for radiolabelling coatings. Instead, the radioactive group is introduced to the coating *via* covalent bond formation. Again, many examples have been reported and we highlight just two representative approaches (Figure 2).

In 2009, Devaraj *et al*. reported the synthesis and multi-modal PET-computed tomography (PET/CT) imaging using ^{18}F-radiolabelled cross-linked dextran iron oxide (CLIO) nanoparticles (*22*). The innovation step in radiolabelling involved derivatisation of the dextran coating with a reactive azide group. Subsequent copper-catalysed azide-alkyne cycloaddition 'Click' reactions using a pre-synthesised ^{18}F-PEG$_3$ alkyne-reagent (produced in an average 57% decay-corrected RCY) facilitated rapid ^{18}F-radiolabelling of azide-functionalised CLIO nanoparticles in 40 min at 40 °C. As with most nanoparticle-based radiotracers, purification from the non-reacted ^{18}F-PEG$_3$-alkyne was achieved by using a simple filtration step to give the final ^{18}F-CLIO product in 58% decay corrected RCY and >99% radiochemical purity. This work showcases the potential of 'Click' chemistry for producing complex radiolabelled constructs in a simple, high yielding and biochemically orthogonal process.

Coating-based metal ion chelation was used by Thorek *et al*. to produce [^{89}Zr]Zirconium-desferrioxamine (DFO) labelled Feraheme® (Ferumoxytol) for use in multi-modal PET/MRI imaging of sentinel lymph nodes (Figure 2) (*23*). In a three-step process the carboxymethyl dextran coating of Feraheme was functionalised with 1,2-ethylenediamine followed by conjugation to DFO-pBn-SCN and subsequent radiolabelling with ^{89}Zr-oxalate to produce ^{89}Zr-DFO-Feraheme. Subsequent PET/MRI imaging in a transgenic mouse model of prostate cancer displaying elevated levels of MYC transcription factor activity showed localisation of ^{89}Zr-DFO-Feraheme in prostate-draining lymph nodes. Whilst this DFO-based method to radiolabel Feraheme with ^{89}Zr was recently superseded by a chelate-free approach (*vide infra*) (*24*), this study provides a convincing demonstration of the need for multi-modal PET/MRI of deep-seated tissues that are difficult to identify and characterise using single modality cameras.

Non-classical Radiolabelling Methods

A disadvantage of classical radiolabelling methods is that the introduction of a prosthetic group or metal ion chelate can have adverse effects on the pharmacokinetic and toxicity profiles of the nanoparticle (*6*,*7*). For this reason, efforts have been made to identify alternative methods for radiolabelling nanoparticles that avoid the use of often bulky, lipophilic prosthetic groups or chelates that alter surface charge (Figure 3).

Radiochemical Doping. This non-classical approach has previously been described as the addition of 'hot-plus-cold' precursors (*11*,*25*). A scientifically more accurate description is 'radiochemical doping' – defined here as a process in which radiolabelled nanoparticles (or more general composites) are made *via* the addition of small amounts of a radionuclide during particle fabrication (Figure 4). The method draws on well-established protocols that have their origins in the Fajans-Paneth-Hahn law of radioactive co-precipitation (see Otto Hahn, 'Applied Radiochemistry' 1936, London, Oxford University Press). The law governs how a radioactive trace element co-precipitates in the presence of a larger amount of carrier material. If experimental conditions including (among others) solubility, concentrations of precipitants, ionic strength and counter ion identity are controlled, then it is possible to generate so-called 'mixed crystals' in which the trace radionuclide is incorporated into the crystal structure of the particulate. Notably, the law also states that if particles acquire a surface charge that is opposite to the charge on the trace element, then co-precipitation of the radioactivity will depend strongly on the conditions used with the tracer likely to become chemically or physically adsorbed onto the particle surface (*vide infra* the sections on chemisorption and physisorption).

Numerous reports using co-precipitation have proven that radiochemical doping is an effective means for generating a wide range of radiolabelled nanoparticles involving different core materials and radionuclides. Radiochemical doping has been achieved using ^{64}Cu (*26–30*), ^{65}Zn (*31*), ^{68}Ga (*32*), ^{109}Cd (*33*), ^{111}In (*31*,*34*), ^{141}Ce (*31*), ^{153}Sm (*35*) and ^{198}Au (*36*,*37*) radionuclides to produce multi-modality particles.

In a state-of-the-art example of homo-radionuclide doping, Black *et al*. produced a range of shape- and size-controlled PEGylated gold nanostructures loaded with ^{198}Au ($t_{1/2}$ = 2.69 d; β^- 100%). All nanoparticles were of a similar size but the authors produced different nanostructures including nanospheres, nanodiscs, nanorods, and cubic nanocages. A combination of *ex vivo* biodistribution data and *in vivo* SPECT coupled with Cerenkov luminescent imaging (CLI) and computed tomography (CT) was used to measure tumour localisation in mice bearing a murine EMT6 breast carcinoma model. Remarkably, pharmacokinetic profiles and intratumoural studies showed that radiotracer distribution was heavily dependent on the particle shape. The ^{198}Au-nanospheres showed the longest blood pool residence time and the highest uptake in tumours reaching 23.2 %ID/g at 24 h. Understanding how the physical shape of nanoparticles influences their behaviour *in vivo* is an emerging frontier in nanoscience that will likely impact future design of multi-modality radiotracers (*38*).

It is important to note that, while radiochemical doping is a fairly general synthetic strategy, not all metal ions and metal-based nanoparticles are compatible. For example, Zeng *et al*. studied the properties of ^{111}In- and ^{57}Co-doped PEGylated Fe_3O_4 nanoparticles. Radiochemical stability measurements found that ^{111}In-doped nanoparticles remained intact at pH2. However, 21.0% of the radioactivity was leached from the ^{57}Co-doped nanoparticles after dialysis for 24 h in water. The difference in the dopant leaching was attributed to the different solubility products of the

corresponding hydroxides (2×10^{-16} for $Co(OH)_2$ and 1.3×10^{-37} for $In(OH)_3$). This work provides important lessons that dopant-nanoparticle chemistry must be matched, and that careful stability measurements should always be performed prior to conducting biological assays *in vitro* and *in vivo*.

Physisorption. While doping involves incorporation of the tracer into the core of the nanoparticle crystal, most other non-classical nanoparticle radiolabelling methods make use of surface-based chemistry. Physical adsorption (physisorption) is a process by which small molecules or ions interact and associate with a molecular surface *via* electrostatic attraction or van der Waals interactions. The key feature of physisorption is that no discrete covalent or dative covalent bond is made between the species binding to the particle and the surface itself. Solid nanoparticles dispersed as a colloid in solution typically acquire a surface charge known as the electric double layer potential (Figure 5). This charged layer is often characterized by the measured zeta potential (in units of mV) with higher net charges (either positive or negative) correlating with increased stability of the colloid in solution and lower net charges favouring coagulation or flocculation. The zeta potential also affects absorption, distribution, metabolism, excretion and toxicological (ADME-tox) properties of nanoparticles (*39*,*40*).

From a radiolabelling perspective, species (ions) that acquire the opposite charge to that of the nanoparticle surface can become immobilised in the stationary layer between the particle surface and the dispersed medium. To the best of our knowledge, there are no specific reports of radiolabelling nanoparticles *via* a physisorption process. However, the absence of data likely reflects our limited mechanistic knowledge on the interactions between radiometal ions with particle surfaces. Many nanoparticle-based systems acquire a negative zeta potential, and hence,

it is intuitive that positively charge metal cation species can potentially form a tight ion pair with the surface and become 'trapped' electrostatically in the immobile region. Further studies are required to elucidate if physisorption is a viable method for radiolabelling nanoparticles.

Direct Chemisorption. Arguably the most versatile and promising new method for radiolabelling a broad scope of nanoparticles involves direct chemical bond formation between the radionuclide and the particle surface (Figure 3). In surface chemistry, this mechanism is called chemisorption. The approach was pioneered by the group of Weibo Cai and co-workers (*41–48*). The concept has recently been generalised, first by our group (*24*) for metal ions from across the Period Table, and subsequently by others for different classes of nanoparticle (*49–52*).

In 2013, Chen *et al.* reported an intriguing study in which the well-known affinity of As^{3+} and As^{5+} ions for the surface of magnetite (Fe_3O_4) was exploited to develop a novel chelate-free approach for producing *As-radiolabelled superparamagnetic iron oxide nanoparticles (*As-SPIONs, where * = 71, 72, 74, 76) as potential PET/MRI imaging agents (*41*). The high affinity of arsenic ions for Fe_3O_4 has been attributed to direct chemisorption in which $As^{3+}O_3$ trigonal pyramids or $As^{5+}O_4$ tetrahedra occupy vacant FeO_4 tetrahedral sites on the octahedrally terminated {111} surface of the magnetite nanoparticles. Control studies using citrate-capped copper sulfide (CuS) nanoparticles or SPIONs coated with dense silica ($dSiO_2$) showed no appreciable radiolabelling confirming that the adsorption process involved specific chemical interactions with the magnetite surface. Further studies in mice demonstrated that the PEGylated compounds, *As-SPION-PEG, were suitable radiotracers for mapping lymph-node drainage with PET/MRI. It is noteworthy that prior to the development of this chelate-free method, chemical options for radiolabelling molecules with $*As^{n+}$ were restricted to As-thiolate chelation. Follow-up studies

have found that direct chemisorption is a viable synthetic route for producing multi-modality radiotracers using different radionuclides (^{69}Ge, ^{64}Cu, ^{89}Zr and recently ^{45}Ti) and nanoparticles including SPIONs, iron oxide-coated MoS_2 nanosheets, mesoporous silica nanoparticles (MSNs), Gd_2O_2S:Eu nanophosphors, and nanographene.

In 2015, our group demonstrated the generality of chelate-free chemisorption radiolabelling of iron oxide-based nanoparticles (*24*). Non-radioactive induction-coupled plasma mass spectrometry studies found that chemisorption could be used to label Feraheme (FH) nanoparticles with different metal ions including *p*-block In^{3+}, first row *d*-block Mn^{2+}, Co^{2+}, Cu^{2+} and Zn^{2+}, second row Zr^{4+}, and *f*-block lanthanide ions like Eu^{3+} and Tb^{3+} (Figure 6A). Radiolabelling experiments using $^{64}CuCl_2$, $^{111}InCl_3$ and ^{89}Zr-oxalate demonstrated that by using the *same* reaction conditions radiolabelled ^{64}Cu-FH, ^{111}In-FH and ^{89}Zr-FH could be produced in 66±6%, 91±2% and >95% decay corrected radiochemical yields, respectively. This is a remarkable result given the differences in charge, ionic radius, and chemical requirements of these metal ions. *In vitro* characterisation experiments found that the FH nanoparticles were physically and chemically unchanged after radiolabelling and that the radioactivity remained tightly bound to the particles even in the presence of standard chelate challenge or serum stability assays. In most instances, the precise nature and location of the metal ion binding to the particle is not known. However, electron paramagnetic resonance (EPR) studies using natural $^{63/65}$Cu-FH provided a strong indication that the metal ions are surface bound and do not interact with the core crystal structure of the magnetite SPIONs. Further studies are required to elucidate the precise nature of the chemical interactions between different metal ions and different surfaces. PET/MRI and CT imaging experiments were performed using ^{89}Zr-FH which showed that the radiotracer is

potentially useful for monitoring acute phase response inflammation (*via* accumulation in macrophages) or for detecting biochemical changes in the lymphatic system (Figures 6B and 6C).

Subsequent work by Shaffer *et al*. also showed that direct chemisorption using ^{64}Cu, ^{68}Ga, ^{89}Zr, ^{90}Y, ^{111}In and ^{177}Lu was applicable for radiolabelling silica nanoparticles (*49*). Further examples of direct chemisorption include the interaction of $^{89}Zr^{4+}$ ions with phosphate groups of pre-formed liposomes (*53*), ^{18}F-radiolabelling of Al_2O_3-coated $MnFe_2O_4$ and Fe_3O_4 nanoparticles (*54*), ^{18}F-radiolabelling of rare-earth nanoparticles (*55*,*56*) and [^{11}C]methyl iodide radiolabelling of carboxylate- and amine-coated iron oxide nanoparticles (*57*). Collectively, reports on radiolabelling *via* direct chemisorption offer general lessons that, *i*) chelate-free methods typically do not disrupt the physical and biochemical properties of the nanoparticle, and *ii*) the radionuclide-surface chemistry must be well-matched for specific and stable bonding to occur.

Isotope Exchange. Substitution of a non-radioactive nuclide for a chemically equivalent radioactive nuclide is termed isotopic exchange. The method is most frequently encountered in the chemistry of ^{19}F/^{18}F-exchange for radiolabelling small-molecules. A limited number of studies that fall into this category of non-classical radiolabelling of nanoparticles have been reported, but the approach is feasible. For example, Cui *et al*. (*56*) and Sun *et al*. (*55*) evaluated the properties of various ^{18}F-radiolabelled nanoparticles that incorporate $NaYF_4$. At present, it remains unclear if the high affinity of ^{18}F-fluoride anions for $NaYF_4$ surfaces involves a mechanistic addition (chemisorption) or a substitution (isotopic exchange). Nevertheless, as the diversity of nanoparticle-based radiotracers expands, simple isotopic exchange reactions may become more prevalent routes for radiolabelling.

Cation Exchange. The concept of cation exchange is an established process in nanocrystal synthesis and materials science (*58*). Mechanistically, cation exchange is related to the aforementioned isotopic exchange in that a substitution reaction occurs either on the surface or inside the core of the nanocrystal (Figure 3). The key difference is that for cation exchange, the incoming radionuclide and the displaced cation can be chemically distinct. Perhaps the term 'heteronuclide exchange' is a more appropriate since it encompasses possible substitution of different atoms, irrespective of the charge. To the best of our knowledge, only two reports that have utilized cation exchange for radiolabelling nanoparticles.

Sun *et al*. produced ^{64}Cu-radiolabelled CdSe/ZnS quantum dots (QDs) *via* M^{2+} cation exchange (*59*). The process was described as 'doping' but since the QDs were pre-fabricated prior to radiolabelling, the mechanism is more accurately classified as cation exchange or chemisorption. Interestingly, incorporation of ^{64}Cu-radionuclides into the QDs induced the particles to 'auto-fluoresce' after excitation from the emitted Cerenkov radiation. Subsequent measurements in mice bearing U87MG glioblastoma model showed specific accumulation of ^{64}Cu-QDs in the tumours and provided evidence that optical luminescence imaging can be fused with nuclear imaging in the form of multi-modality PET/CLI.

Separately, Sun *et al*. (*60*) reported that cation exchange could be used to radiolabel different mixed core-shell nanoparticles based on $NaLuF_4$:Yb,Gd,Tm composites with ^{153}Sm. This example lies at the borderline between cation exchange and radiochemical doping (*35*). The authors produced a composite nanoparticle consisting of a $NaLuF_4$:Yb,Tm coated in a secondary shell of $NaGdF_4$(^{153}Sm). A homogenous solution of $GdCl_3$ and $^{153}SmCl_3$ was added to pre-formed nanocrystals of $NaLuF_4$ to form a radiolabelled coating using forcing conditions. Subsequent annealing at 300 °C and re-dispersion in citrate produced cit-$NaLuF_4$:Yb,Tm@$NaGdF_4$(^{153}Sm)

nanocrystals. While successful in the production of a multi-modality optical/SPECT/CT imaging agent, such harsh radiolabelling conditions will limit potential biomedical applications of this method.

Particle Beam or Reactor Activation. An interesting concept toward radiolabelled nanoparticles is to pre-synthesise the non-radioactive variant and then use particle beam or reactor-based activation to transmute an atom *in situ* (*5*) (Figure 3). Both neutron (*61*,*62*) and proton (*63*,*64*) activations have been reported to produce radiolabelled nanoparticles *via* $^{18}O(p,n)^{18}F$, $^{16}O(p,\alpha)^{13}N$, and $^{165}Ho(n,\gamma)^{166}Ho$ transmutation. For example, Munaweera *et al*. produced ^{166}Ho-radiolabelled garnet nanoparticles loaded with various platinum-based chemotherapeutics (*62*). The magnetic ^{166}Ho-HolG-Pt were selectively delivered to a lung tumour model using an external magnetic field. Statistically significant decreases in tumour burden were noted for groups treated with both active Pt complexes and the application of an external magnetic field *versus* controls. While this inorganic system shows promise, lack of stability of organic materials in the particle beam will likely limit more wide-spread use of this method.

Cavity Encapsulation. The final method involves trapping a radioactive species inside the cavity of a nanoparticle. The process relies on a physical encapsulation which can also be described as a 'mechanical bond'. Classic examples of systems that allow for drug encapsulation include liposomes (*65*) and single-walled carbon nanotubes (SWCNTs) (*66*) (Figure 7). While incorporation of radiometal ions into the aqueous phase core of liposomes is a well-established method for producing radioscintigraphy and SPECT imaging agents using ^{99m}Tc, insertion of radionuclides into nanotubes is more challenging. In 2014, Cisneros *et al*. reported methods for

the stable, simultaneous confinement of both Gd^{3+} ions and $^{64}Cu^{2+}$ ions into ultra-short SWCNTs (*66*). Radiolabelled nanotubes were stabilised using surfactants and although some ^{64}Cu was removed by serum challenge, the constructs were sufficiently stable to allow evaluation of the pharmacokinetic profiles using PET/MRI. Since SWCNTs have a high loading capacity, and the Gd^{3+} ions and radionuclides contained within are shielded from the biological environment, cavity encapsulation offers a potential solution for solving the concentration problem between PET and MRI without compromising biological specificity.

CONCLUSIONS

Emerging methods that exploit the intrinsic chemical and physical properties of nanoparticles have sparked a revolution in surface-based radiochemistry. While nanoparticles remain inherently challenging systems, they present unparalleled opportunities for developing multi-modality radiotracers. A switch to chelate-free radiochemistry has broadened the tools available to radiochemists, narrowing the gap between academic curiosity and clinical translation. Future advancements will likely ultilise intrinsically labelled nanomedicines as multi-modal imaging agents that target specific disease biomarkers.

ACKNOWLEDGMENTS

JPH thanks the Swiss National Science Foundation (SNSF Professorship PP00P2_163683), the European Research Council (ERC-StG-2015, NanoSCAN – 676904), and the University of Zurich for funding.

REFERENCES

1. Wagner V, Dullaart A, Bock AK, Zweck A. The emerging nanomedicine landscape. *Nat Biotechnol*. 2006;24:1211-1217.

2. Welch MJ, Hawker CJ, Wooley KL. The advantages of nanoparticles for PET. *J Nucl Med*. 2009;50:1743-1746.

3. Liu Y, Welch MJ. Nanoparticles labeled with positron emitting nuclides: advantages, methods, and applications. *Bioconjug Chem*. 2012;23:671-682.

4. Xing Y, Zhao J, Conti PS, Chen K. Radiolabeled nanoparticles for multimodality tumor imaging. *Theranostics*. 2014;4:290-306.

5. Zhao J, Zhou M, Li C. Synthetic nanoparticles for delivery of radioisotopes and radiosensitizers in cancer therapy. *Cancer Nanotechnol*. 2016;7:9.

6. Rivera-Gil P, Jimenez de Aberasturi D, Wulf V, et al. The challenge to relate the physicochemical properties of colloidal nanoparticles to their cytotoxicity. 2012;46:743-749.

7. Hong H, Chen F, Cai W. Pharmacokinetic issues of imaging with nanoparticles: focusing on carbon nanotubes and quantum dots. *Mol Imaging Biol*. 2013;15:507-520.

8. Lapi SE, Welch MJ. A historical perspective on the specific activity of radiopharmaceuticals: what have we learned in the 35 years of the ISRC? *Nucl Med Biol*. 2012;39:601-608.

9. Schühle DT, Caravan P. Metal-Based MRI Contrast Agents. Vol II. Charlestown: Elsevier; 2013;901-932.

10. Zhao Y, Liang M, Li X, et al. Bioengineered magnetoferritin nanoprobes for single-dose nuclear-magnetic resonance tumor imaging. *ACS Nano*. 2016;10:4184-4191.

11. Goel S, Chen F, Ehlerding EB, Cai W. Intrinsically radiolabeled nanoparticles: an emerging paradigm. *Small*. 2014;10:3825-3830.

12. Sun X, Cai W, Chen X. Positron emission tomography imaging using radiolabeled inorganic nanomaterials. *Acc Chem Res*. 2015;48:286-294.

13. Stockhofe K, Postema JM, Schieferstein H, Ross TL. Radiolabeling of nanoparticles and polymers for PET imaging. *Pharmaceuticals*. 2014;7:392-418.

14. Unak G, Ozkaya F, Ilker Medine E, et al. Gold nanoparticle probes: design and in vitro applications in cancer cell culture. *Colloids Surfaces B Biointerfaces*. 2012;90:217-226.

15. Guerrero S, Herance JR, Rojas S, et al. Synthesis and in vivo evaluation of the biodistribution of a ^{18}F-labeled conjugate gold-nanoparticle-peptide with potential biomedical application. *Bioconjug Chem*. 2012;23:399-408.

16. Zhu J, Chin J, Wängler C, Wängler B, Lennox RB, Schirrmacher R. Rapid ^{18}F-labeling and loading of PEGylated gold nanoparticles for in vivo applications. *Bioconjug Chem*.

2014;25:1143-1150.

17. Rojas S, Gispert JD, Abad S, et al. In vivo biodistribution of amino-functionalized ceria nanoparticles in rats using positron emission tomography. *Mol Pharm*. 2012;9:3543-3550.

18. Torres Martin de Rosales R, Tavaré R, Paul RL, et al. Synthesis of $^{64}Cu^{II}$-bis(dithiocarbamatebisphosphonate) and its conjugation with superparamagnetic iron oxide nanoparticles: In vivo evaluation as dual-modality PET-MRI agent. *Angew Chemie - Int Ed*. 2011;50:5509-5513.

19. Torres Martin de Rosales R, Tavaré R, Glaria A, Varma G, Protti A, Blower PJ. 99m Tc-bisphosphonate-iron oxide nanoparticle conjugates for dual-modality biomedical imaging. *Bioconjug Chem*. 2011;22:455-465.

20. Gaynor D, Griffith DM. The prevalence of metal-based drugs as therapeutic or diagnostic agents: beyond platinum. *Dalt Trans*. 2012;41:13239.

21. Sandiford L, Phinikaridou A, Protti A, et al. Bisphosphonate-anchored pegylation and radiolabeling of superparamagnetic iron oxide: long-circulating nanoparticles for in vivo multimodal (T1 MRI-SPECT) imaging. *ACS Nano*. 2013;7:500-512.

22. Devaraj NK, Keliher EJ, Thurber GM, Nahrendorf M, Weissleder R. ^{18}F labeled nanoparticles for in vivo PET-CT imaging. *Bioconjug Chem*. 2009;20:397-401.

23. Thorek DLJ, Ulmert D, Diop N-FM, et al. Non-invasive mapping of deep-tissue lymph nodes in live animals using a multimodal PET/MRI nanoparticle. *Nat Commun*. 2014;5;3097.

24. Boros E, Bowen AM, Josephson L, Vasdev N, Holland JP. Chelate-free metal ion binding and heat-induced radiolabeling of iron oxide nanoparticles. *Chem Sci*. 2015;6:225-236.

25. Goel S, Chen F, Cai W. Synthesis and biomedical applications of copper sulfide nanoparticles: from sensors to theranostics. *Small*. 2014;10:631-645.

26. Zhou M, Zhang R, Huang M, et al. A chelator-free multifunctional [^{64}Cu]CuS nanoparticle platform for simultaneous micro-PET / CT imaging and photothermal ablation therapy. *J Am Chem Soc*. 2010;132:15351-15358.

27. Wong RM, Gilbert DA, Liu K, Louie AY. Rapid size-controlled synthesis of dextran-coated, ^{64}Cu-doped iron oxide nanoparticles. *ACS Nano*. 2012;6:3461-3467.

28. Zhao Y, Sultan D, Detering L, et al. Copper-64-alloyed gold nanoparticles for cancer imaging: improved radiolabel stability and diagnostic accuracy. *Angew Chemie - Int Ed*. 2014;53:156-159.

29. Sun X, Huang X, Yan X, et al. Chelator-free ^{64}Cu-integrated gold nanomaterials for positron emission tomography imaging guided photothermal cancer therapy. 2014;8:8438-8446.

30. Guo W, Sun X, Jacobson O, et al. Intrinsically radioactive [^{64}Cu]CuInS/ZnS quantum dots

for pet and optical imaging: Improved radiochemical stability and controllable cerenkov luminescence. *ACS Nano*. 2015;9:488-495.

31. Yang L, Sundaresan G, Sun M, et al. Intrinsically radiolabeled multifunctional cerium oxide nanoparticles for in vivo studies. *J Mater Chem B*. 2013;1:1421.

32. Pellico J, Ruiz-Cabello J, Saiz-Alía M, et al. Fast synthesis and bioconjugation of ^{68}Ga core-doped extremely small iron oxide nanoparticles for PET/MR imaging. *Contrast Media Mol Imaging*. 2016;11:203-210.

33. Sun M, Hoffman D, Sundaresan G, Yang L, Lamichhane N, Zweit J. Synthesis and characterization of intrinsically radiolabeled quantum dots for bimodal detection. *Am J Nucl Med Mol Imaging*. 2012;2:122-135.

34. Zeng J, Jia B, Qiao R, et al. In situ ^{111}In-doping for achieving biocompatible and non-leachable ^{111}In-labeled Fe_3O_4 nanoparticles. *Chem Commun*. 2014;50:2170-2172.

35. Yang Y, Sun Y, Cao T, et al. Hydrothermal synthesis of $NaLuF_4$:^{153}Sm,Yb,Tm nanoparticles and their application in dual-modality upconversion luminescence and SPECT bioimaging. *Biomaterials*. 2013;34:774-783.

36. Wang Y, Liu Y, Luehmann H, et al. Radioluminescent gold nanocages with controlled radioactivity for real-time in vivo imaging. *Nano Lett*. 2013;13:581-585.

37. Black KCL, Wang Y, Luehmann HP, et al. Radioactive ^{198}Au-doped nanostructures with different shapes for in vivo analyses of their biodistribution, tumor uptake, and intratumoral distribution. 2014;8:4385-4394.

38. Wu Z, Yang S, Wu W. Shape control of inorganic nanoparticles from solution. *Nanoscale*. 2016;8:1237-1259.

39. McNeil SE. Nanoparticle therapeutics: a personal perspective. *Wiley Interdiscip Rev: Nanomed Nanobiotechnol*. 2009;1:264-271.

40. Nel AE, Mädler L, Velegol D, et al. Understanding biophysicochemical interactions at the nano–bio interface. *Nat Mater*. 2009;8:543-557.

41. Chen F, Ellison PA, Lewis CM, et al. Chelator-free synthesis of a dual-modality PET/MRI agent. *Angew Chemie - Int Ed*. 2013;52:13319-13323.

42. Chakravarty R, Valdovinos HF, Chen F, et al. Intrinsically germanium-69 labeled iron oxide nanoparticle: synthesis and in vivo dual-modality PET/MR imaging. *Adv Mater*. 2014;26:5119-5123.

43. Liu T, Shi S, Liang C, et al. Iron oxide decorated MoS_2 nanosheets with double PEGylation for chelator-free radiolabeling and multimodal imaging guided photothermal therapy. 2015;9:950-960.

44. Goel S, Chen F, Luan S, et al. Engineering intrinsically zirconium-89 radiolabeled self-destructing mesoporous silica nanostructures for in vivo biodistribution and tumor

targeting studies. *Adv Sci*. 2016;3:1-11.

45. Ai F, Goel S, Zhan Y, et al. Intrinsically ^{89}Zr-labeled Gd_2O_2S:Eu nanophosphors with high in vivo stability for dual-modality imaging. *Am J Transl Res*. 2016;8:5591-5600.

46. Shi S, Xu C, Yang K, et al. Chelator-free radiolabeling of nanographene: breaking the stereotype of chelation. *Angew Chemie - Int Ed*. 2017;56:2889-2892.

47. Ellison PA, Chen F, Goel S, et al. Intrinsic and stable conjugation of thiolated mesoporous silica nanoparticles with radioarsenic. *ACS Appl Mater Interfaces*. 2017;9:6772-6781.

48. Chen F, Valdovinos HF, Hernandez R, Goel S, Barnhart TE, Cai W. Intrinsic radiolabeling of Titanium-45 using mesoporous silica nanoparticles. *Acta Pharmacol Sin*. 2017;38:907-913.

49. Shaffer TM, Wall MA, Harmsen S, et al. Silica nanoparticles as substrates for chelator-free labeling of oxophilic radioisotopes. *Nano Lett*. 2015;15:864-868.

50. Pham THN, Lengkeek NA, Greguric I, et al. Tunable and noncytotoxic PET / SPECT-MRI multimodality imaging probes using colloidally stable ligand-free superparamagnetic iron oxide nanoparticles. *I J Nano Med*. 2017;12:899-909.

51. Wall MA, Shaffer TM, Harmsen S, et al. Chelator-free radiolabeling of SERRS nanoparticles for whole-body PET and intraoperative raman imaging. *Theranostics*. 2017;7:3068-3077.

52. Radović M, Calatayud MP, Goya GF, et al. Preparation and in vivo evaluation of multifunctional ^{90}Y-labeled magnetic nanoparticles designed for cancer therapy. *J Biomed Mater Res - Part A*. 2015;103:126-134.

53. Abou DS, Thorek DLJ, Ramos NN, et al. ^{89}Zr-labeled paramagnetic octreotide-liposomes for PET-MR imaging of cancer. *Pharm Res*. 2013;30:878-888.

54. Cui X, Belo S, Krüger D, et al. Aluminium hydroxide stabilised $MnFe_2O_4$ and Fe_3O_4 nanoparticles as dual-modality contrasts agent for MRI and PET imaging. *Biomaterials*. 2014;35:5840-5846.

55. Sun Y, Yu M, Liang S, et al. Fluorine-18 labeled rare-earth nanoparticles for positron emission tomography (PET) imaging of sentinel lymph node. *Biomaterials*. 2011;32:2999-3007.

56. Cui X, Mathe D, Kovács N, et al. Synthesis, characterization, and application of core-shell $Co_{0.16}Fe_{2.84}O_4$@$NaYF_4$(Yb, Er) and Fe_3O_4@$NaYF_4$(Yb, Tm) nanoparticle as trimodal (MRI, PET/SPECT, and Optical) imaging agents. *Bioconjug Chem*. 2016;27:319-328.

57. Sharma R, Xu Y, Kim SW, et al. Carbon-11 radiolabeling of iron-oxide nanoparticles for dual-modality PET/MR imaging. *Nanoscale*. 2013;5:7476.

58. Son DH, Hughes SM, Yin Y, Alivisatos AP. Cation exchange reactions in ionic nanocrystals. *Science*. 2004;306:1009-1012.

59. Sun X, Huang X, Guo J, et al. Self-illuminating ^{64}Cu-doped CdSe/ZnS nanocrystals for in vivo tumor imaging. *J Am Chem Soc*. 2014;136:1706-1709.

60. Sun Y, Zhu X, Peng J, Li F. Core-shell lanthanide upconversion nanophosphors as four-modal probes for tumor angiogenesis imaging. *ACS Nano*. 2013;7:11290-11300.

61. Di Pasqua a. J, Yuan H, Chung Y, et al. Neutron-activatable holmium-containing mesoporous silica nanoparticles as a potential radionuclide therapeutic agent for ovarian cancer. *J Nucl Med*. 2013;54:111-116.

62. Munaweera I, Shi Y, Koneru B, et al. Chemoradiotherapeutic magnetic nanoparticles for targeted treatment of nonsmall cell lung cancer. *Mol Pharm*. 2015;12:3588-3596.

63. Pérez-Campaña C, Moya SE, Ziolo RF, et al. Biodistribution of different sized nanoparticles assessed by positron emission tomography : a general strategy for direct activation of metal. *ACS Nano*. 2013;7:3498-3505.

64. Pérez-Campaña C, Gómez-Vallejo V, Martin A, et al. Tracing nanoparticles in vivo: a new general synthesis of positron emitting metal oxide nanoparticles by proton beam activation. *Analyst*. 2012;137:4902.

65. Boerman OC, Laverman P, Oyen WJG, Corstens FHM, Storm G. Radiolabeled liposomes for scintigraphic imaging. *Prog Lipid Res*. 2000;39:461-475.

66. Cisneros BT, Law JJ, Matson ML, Azhdarinia A, Sevick-Muraca EM, Wilson LJ. Stable confinement of positron emission tomography and magnetic resonance agents within carbon nanotubes for bimodal imaging. *Nanomedicine*. 2014;9:2499-2509.

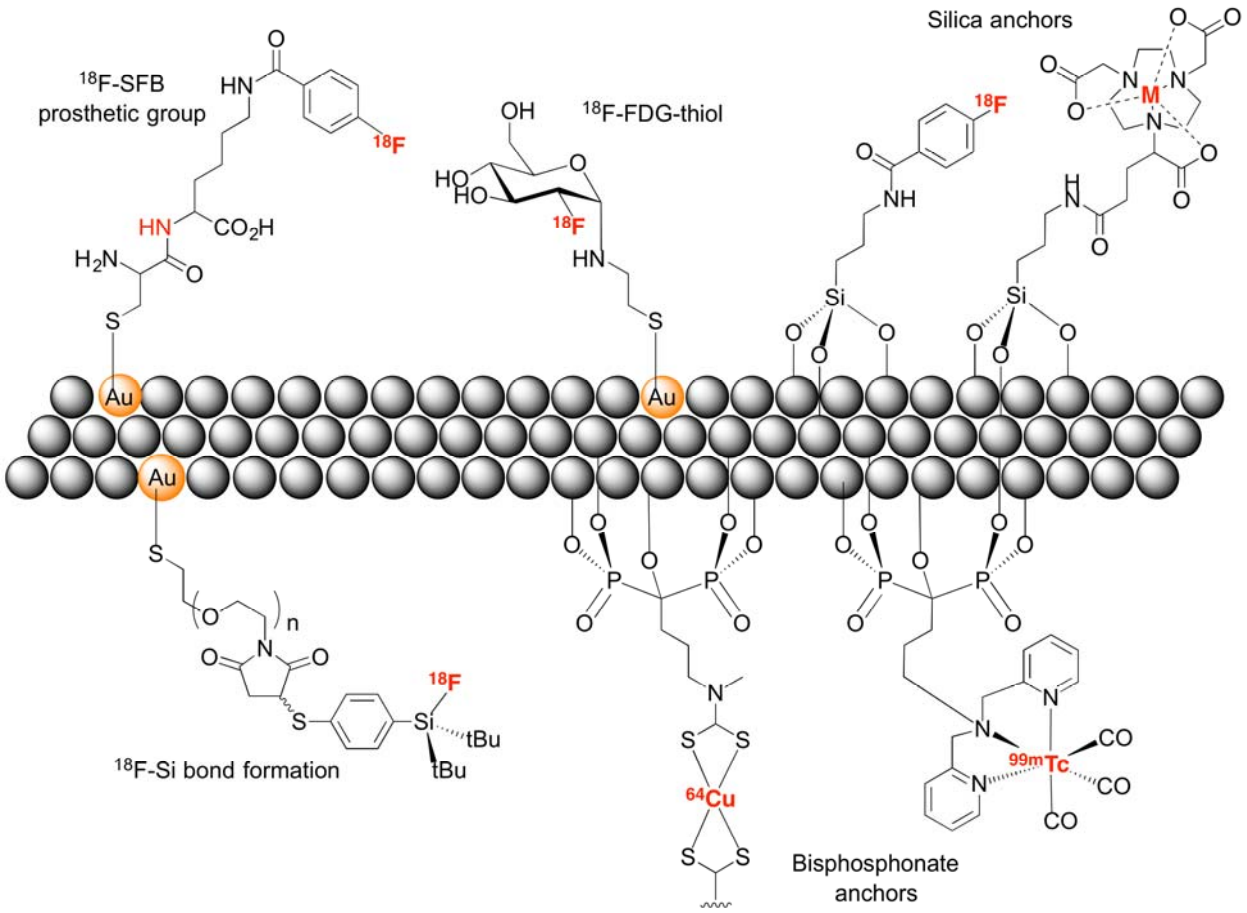

Figure 1. Illustration of some of classical, surface-based methods that have been used to radiolabelled nanoparticles.

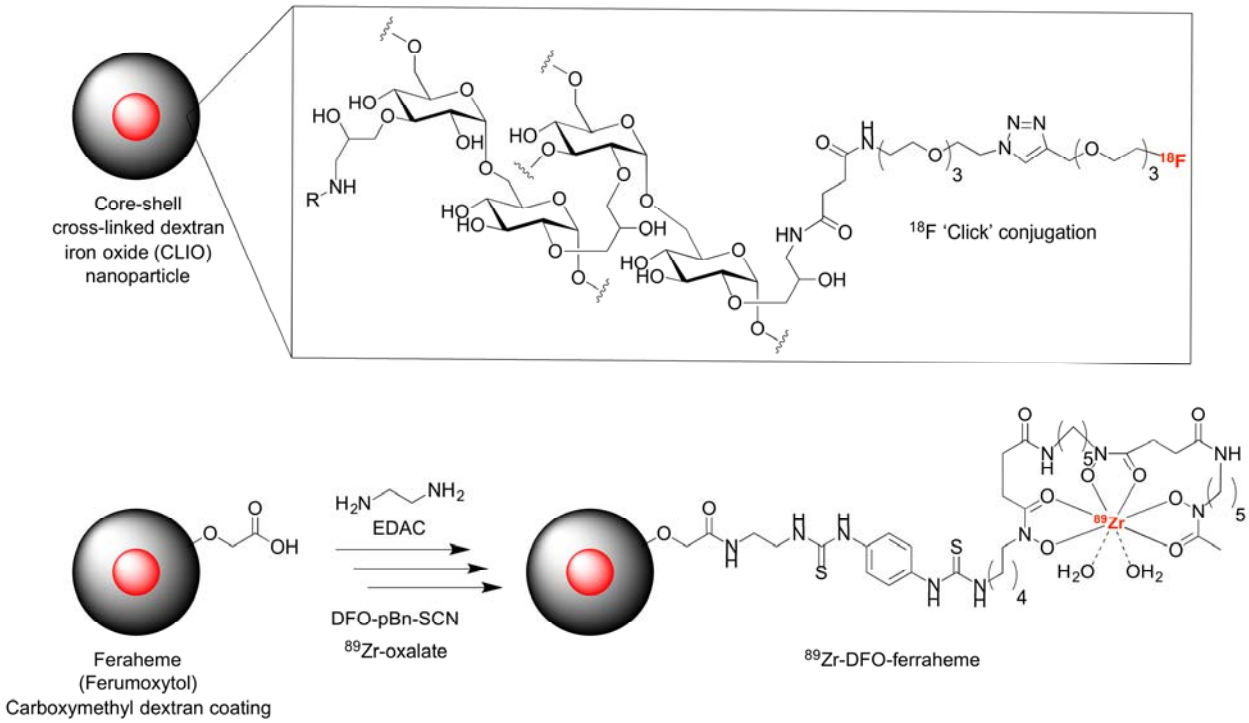

Figure 2. Two prominent examples of classic coating-based radiolabelling methods.

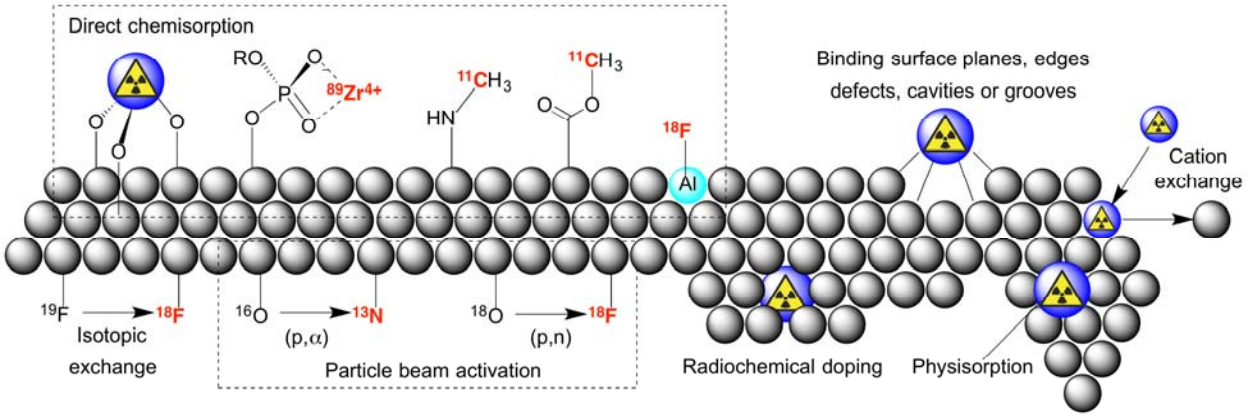

Figure 3. Illustration of the diversity of emerging chelate-free methods that are being developed for radiolabelling different nanoparticles.

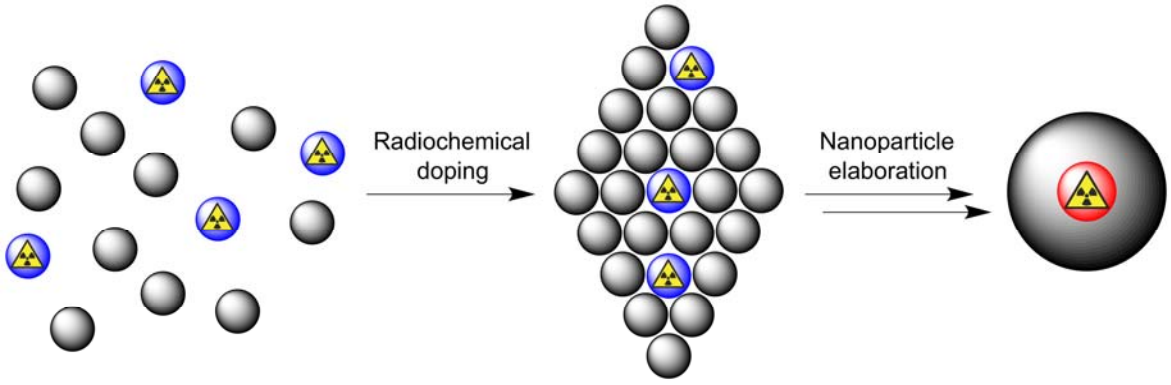

Figure 4. Schematic showing the concept of radiochemical doping during nanoparticle fabrication.

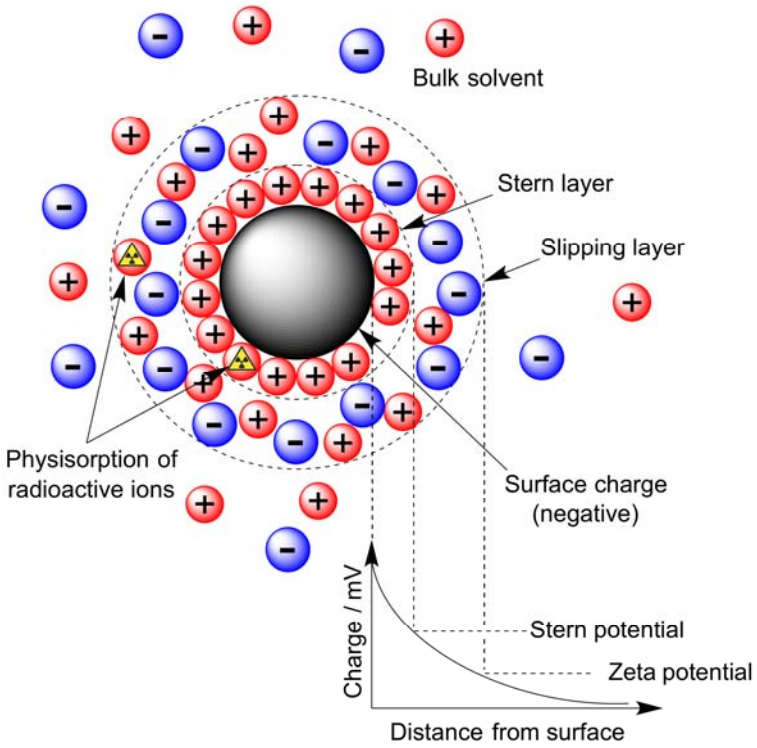

Figure 5. Schematic showing the distribution of charged ions around the surface of a nanoparticle in solution.

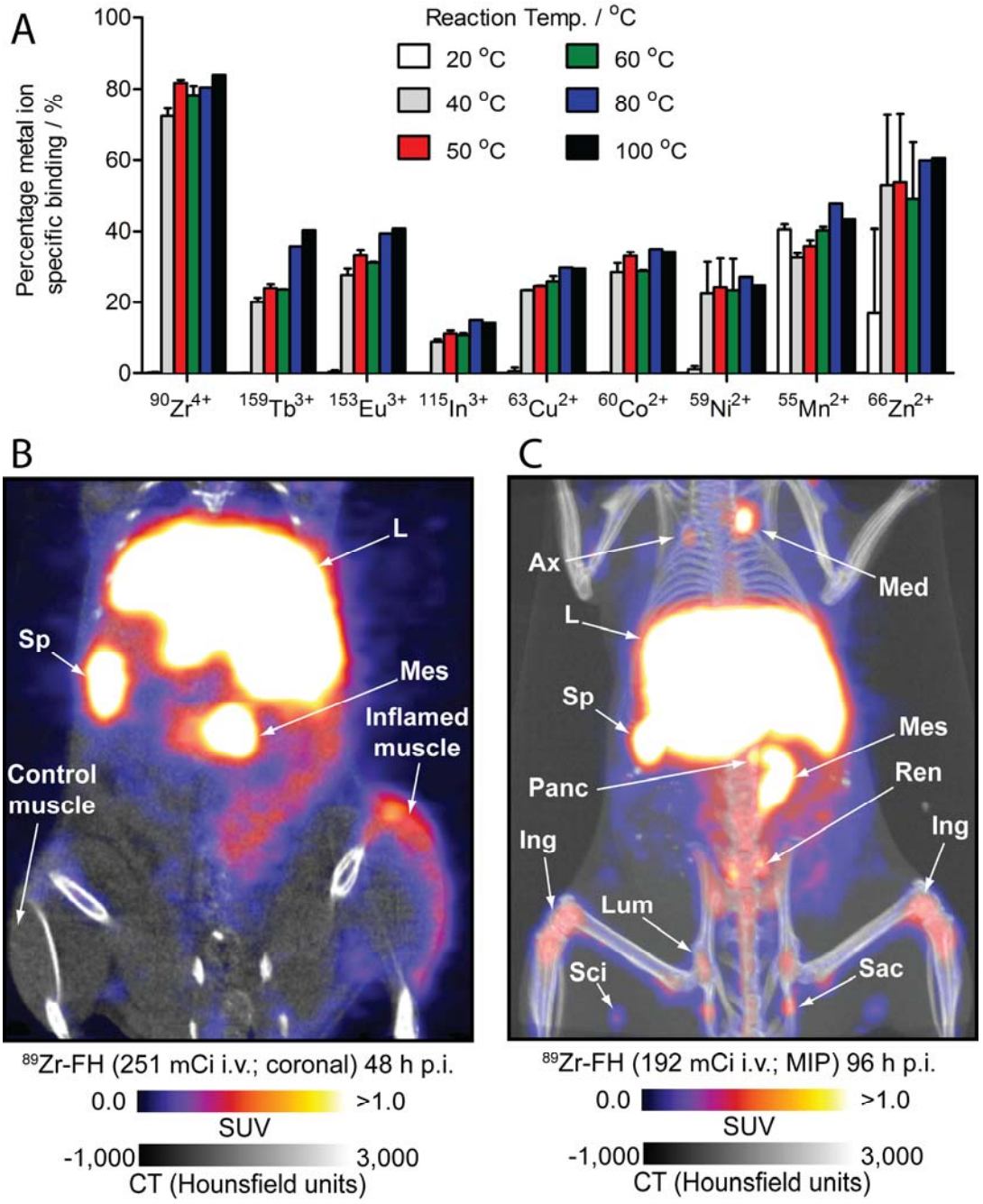

Figure 6. (A) Temperature-dependent induction-coupled plasma mass spectrometry data showing that metal ion salts from across the Periodic Table can be used in chelate-free labelling. PET/CT images showing the uptake of ^{89}Zr-FH in (B) in an acute phase response inflammation model, and (C) normal lymph nodes.

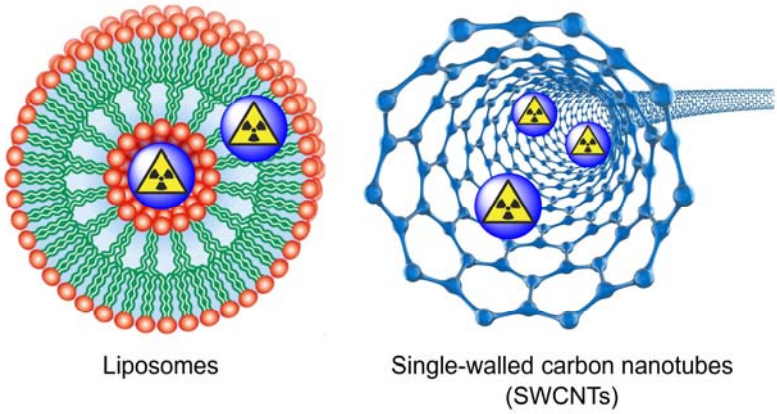

Figure 7. Schematic showing cavity encapsulation of a radiolabel inside liposomes and single-walled carbon nanotubes. The underlying liposome figure has been reproduced under a Creative Commons Attribution: Vladimir P. Shirinsky, http://eng.thesaurus.rusnano.com/wiki/article1075.